

DEUTERON BREAK-UP: THEORETICAL DESCRIPTION OF POLARIZATION OBSERVABLES IN STAPP FORMALISM

O.G.Grebnyuk ^{*}

Petersburg Nuclear Physics Institute, 188350, Gatchina, Russia

Abstract

The vector A_y and tensor A_{yy} analyzing powers as well as the polarization of the outgoing proton are calculated for the exclusive deuteron break-up reaction $\vec{d}p \rightarrow \vec{p}pn$ at a deuteron beam energy of 2 GeV. Two component covariant formalism of Stapp has been used to have the completely Lorentz invariant model. In addition to the Impulse Approximation the nucleon-nucleon double-scattering and delta-excitation mechanism have been added coherently. Good agreement with the precise data obtained at Saclay is achieved .

PACS: 21.45+v, 24.70+s, 25.10+s

Keywords: NUCLEAR REACTION $\vec{d}(p, \vec{p}, p)n$ E=2.0 GeV, calculated vector analyzing power A_y , tensor analyzing power A_{yy} , polarization of the proton, covariant formalism, double-scattering, delta-excitation

^{*}e-mail: olegreb@mail.desy.de

Introduction

The exclusive break-up of the polarized deuteron by the protons at a deuteron beam energy of 2 GeV was studied at Saclay [1, 2]. The experiment was motivated by the idea to explore the important details of the deuteron wave function at the high internal momenta. As compared with the series of previous $dp \rightarrow ppn$ experiments [3, 4, 5, 6, 7], this experiment was designed to be sensitive to the ratio between the S - and D -components of the deuteron wave function brought by polarization observables. The sensitivity to the S/D ratio is maximum when the Impulse Approximation (IA) is valid. In this approximation one of the deuteron's nucleon is a spectator and another one interacts with the beam/target proton. As theory predicts, and it is confirmed experimentally, the IA is valid only when the internal momentum of the deuteron does not exceed ≈ 200 MeV/c. An attempt of straightforward experimental testing of the deuteron wave function above this momentum could be justified only if other mechanisms beyond of the IA are well under the control. Therefore a good knowledge of other interaction mechanisms is of the great importance in the experiments of such kind.

That is why the theory of the correction to the IA has a history as long as the experiments initiated by this approximation. Chew and Goldberger [8] represented the scattering of the elementary particles by complex nuclei as the multiple-scattering series $T = \sum_{k=1}^{\infty} T^{(k)}$, where k is the number of two-body NN interactions. The $T^{(1)}$ corresponds to the single-scattering and contains the IA term, $T^{(2)}$ corresponds to the double-scattering and so on. Analogous development follows from the Faddeev equations [9]. Everett [10] was the first who scrutinized the double-scattering terms. He used the spin-dependent NN am-

plitude from the phase shift analysis (PSA) corrected so as to allow one nucleon to be off-shell and calculated the loop integrals of the double-scattering graphs, taking the NN amplitudes out of the integral at a fixed point. Golovin et al. [11] used the similar method with the up-date NN amplitudes.

Another approach was developed by Wallace [12]. He took an advantage of the Glauber cancellation by the high-order terms in multiple-scattering series of those pieces of the double-scattering loop integral, which originate from off-shell states [13]. This approach obtained an application by Punjabi et al. [14].

The question about the role of the Δ -isobar in the (p,2p)-reactions often arises when discussing the discrepancies between the experiment data and predictions with the only NN rescatterings. Yano [15] calculated the contribution of the Δ -isobar to the deuteron break-up reaction using Feynman diagram approach but the corresponding amplitude was added incoherently to the other amplitudes.

The analysis of the copious and precise data on the polarization parameters in exclusive $\vec{d}p \rightarrow \vec{p}pn$ reaction, obtained at Saclay [2], requires to deal with the interference between the various amplitudes of the multiple scattering. In this paper we present such a model. It is based on the approach of Everett and includes the spin and isospin variables. The model takes into account the double-scattering contribution and also the graphs including the process $\pi^*d \rightarrow NN$, the virtual pion being emitted by the beam/target proton. Since the $\pi d \rightarrow NN$ reaction at these energies goes mainly through ΔN in the intermediate state, the graphs considered by Yano are also added in a coherently to the other contributions. Furthermore, the pion-nucleon scattering in other partial waves (S, P, D) is also considered.

When calculating the nucleon-nucleon rescattering contributions to the deuteron break-up amplitude one needs to transform the NN matrices from nucleon-nucleon center of mass frames to the common laboratory frame. These transformations depend on the spin basis chosen for the one-nucleon states. Usually the canonical or helicity basis are used which are transformed with unitary two by two matrices depending on a nucleon momentum. They are so called Wigner rotations and one needs to make the four different rotations corresponding to the two incoming and two outgoing scattering nucleons. The covariant basis [16, 17] transforming independently of the particle momentum by the unimodular two by two matrices is free from this deficiency. An amplitudes in the covariant basis are usually referred to as the M-functions of Stapp. The covariant formalism of the M-functions developed by Stapp [17, 18] is based on the matrices $\sigma^\mu = (1, \vec{\sigma})$ and $\tilde{\sigma}^\mu = (1, -\vec{\sigma})$, where $\vec{\sigma}$ are the standard Pauli matrices. With an each kinematical momentum P^μ of the reaction two by two matrices $\tilde{P} \equiv P^\mu \tilde{\sigma}_\mu$ and $P \equiv P^\mu \sigma_\mu$ are associated. The products $\tilde{P}_i P_j$ of these matrices are the elements from which the M-functions are built. The matrices \tilde{V}_i and V_i associated with the four-velocity of the i-th particle, serve as the metric tensors of the particle when performing the contraction over this index (traces, successive processes).

The outline of the paper is as follows. The Sections 1-3 cover the three main mechanisms involved in the deuteron break-up: Impulse Approximation, NN double-scattering and Δ -excitation. The polarization observables obtained with the covariant deuteron density matrix are described in the Section 4. The discussion of the calculation results and summary is given in the Section 5. The introduction to the covariant formalism of the M-functions

is given in the Appendix.

1 Impulse Approximation

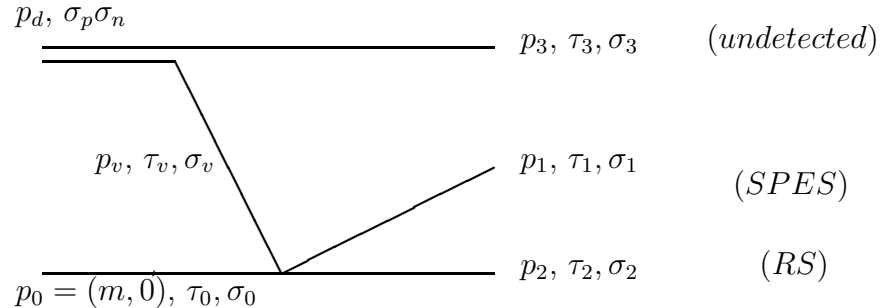


Figure 1: IA mechanism. In Saclay experiment p_1 was measured by the magnetic spectrometer SPES-4 in coincidence with the recoil protons (p_2) detected by Recoil Spectrometer RS.

The general expression for the S -matrix elements of the deuteron break-up reaction is

$$S = i(2\pi)^4 \delta^4(p_1 + p_2 + p_3 - p_0 - p_d) M ,$$

where M is the amplitude of the reaction and we assign indices for the each particle of the reaction $d(p, 2p)n$ as

$$\begin{array}{ccccccc} d & + & p & \rightarrow & p & + & p & + & n \\ (d) & + & (0) & \rightarrow & (1) & + & (2) & + & (3) \end{array} .$$

To avoid in what follows the numerous repetitions of the summation sign Σ , which is inevitable when considering the spin and isotopic spin variables, we will use the tensor-like notation with the indices characterizing spin and isotopic spin projections. The upper and lower indices relate to the final and initial channels, respectively. The same index at the up and down positions stands for a summation over this index. Free nucleon is characterized by the projections of the spin σ , of the isospin τ and by the momentum p . We will use the representation of the deuteron spin states by the symmetric spin-tensor $S^{\sigma_n \sigma_p}$ so that the amplitudes of the reaction with participation of the deuteron will have the pair of indices $\sigma_n \sigma_p$ and will be symmetric with respect to their interchange.

The amplitude of the deuteron break-up reaction with the all indices looks like

$$M_{\tau_0}^{\tau_1 \tau_2 \tau_3; \sigma_1 \sigma_2 \sigma_3} (p_1, p_2, p_3; p_0, p_d) .$$

The Pauli principle requires that this amplitude should be antisymmetric with respect to the interchange of any two final nucleons. For example

$$M_{\tau_0}^{\tau_1 \tau_2 \tau_3; \sigma_1 \sigma_2 \sigma_3} (p_1, p_2, p_3; p_0, p_d) = -M_{\tau_0}^{\tau_2 \tau_1 \tau_3; \sigma_2 \sigma_1 \sigma_3} (p_2, p_1, p_3; p_0, p_d) .$$

To fulfill this requirement we proceed as follows. Having written the expression antisymmetric with respect to the interchange of for example the first and the second nucleons $M^{(12)3}$, we perform then the cyclic permutation of the nucleons. The resulting expression $M^{(12)3} + M^{(23)1} + M^{(31)2}$ possess the required antisymmetry.

Let us start with the expression corresponding to the graph

pictured in Fig. 1. With the all indices it looks like

$$M_{NN}^{\tau_1\tau_2;\sigma_1\sigma_2}(p_1, p_2; p_0, p_v) \frac{i}{2m_v(m_v - m)} D^{\tau_v\tau_3;\sigma_v\sigma_3}_{\sigma_p\sigma_n}(p_v, p_3; p_d) , \quad (1)$$

where $m_v^2 \equiv (p_d - p_3)^2$ is the squared mass of the virtual nucleon and M_{NN} and D are the nucleon-nucleon amplitude and the deuteron vertex, respectively. The above expression corresponds only to the first term in the development of the spinor particle propagator in the Dirac particle-antiparticle formalism

$$\frac{\not{p} + m}{s - m^2} = \frac{1}{2W} \left[\frac{u \cdot \bar{u}}{W - m} - \frac{v \cdot \bar{v}}{W + m} \right] , \quad W = \sqrt{p^2} .$$

Thus we do not consider in what follows the virtual antinucleon states, which requires a knowledge of the antinucleon components of the nucleon-nucleon amplitude and of the deuteron vertex. The deuteron wave function is a product of the vertex and the propagator

$$\frac{D^{\tau_v\tau_3;\sigma_v\sigma_3}_{\sigma_p\sigma_n}(p_v, p_3; p_d)}{2m_v(m_v - m)} \equiv \epsilon^{\tau_v\tau_3} \Phi^{\sigma_v\sigma_3}_{\sigma_p\sigma_n}(p_v, p_3; p_d) , \quad (2)$$

where ϵ is an antisymmetric two by two tensor in isotopic space. The fully antisymmetrized 'one nucleon exchange' (ONE) amplitude is equal to

$$\begin{aligned} M_{ONE}^{\tau_1\tau_2\tau_3;\sigma_1\sigma_2\sigma_3}_{\tau_0;\sigma_0\sigma_p\sigma_n}(p_1, p_2, p_3; p_0, p_d) = \\ i[M_{NN}^{\tau_1\tau_2;\sigma_1\sigma_2}_{\tau_0\tau_v;\sigma_0\sigma_v}(p_1, p_2; p_0, p_d - p_3) \epsilon^{\tau_v\tau_3} \Phi^{\sigma_v\sigma_3}_{\sigma_p\sigma_n}(p_d - p_3, p_3; p_d) + \\ M_{NN}^{\tau_2\tau_3;\sigma_2\sigma_3}_{\tau_0\tau_v;\sigma_0\sigma_v}(p_2, p_3; p_0, p_d - p_1) \epsilon^{\tau_v\tau_1} \Phi^{\sigma_v\sigma_1}_{\sigma_p\sigma_n}(p_d - p_1, p_1; p_d) + \\ M_{NN}^{\tau_3\tau_1;\sigma_3\sigma_1}_{\tau_0\tau_v;\sigma_0\sigma_v}(p_3, p_1; p_0, p_d - p_2) \epsilon^{\tau_v\tau_2} \Phi^{\sigma_v\sigma_2}_{\sigma_p\sigma_n}(p_d - p_2, p_2; p_d)] , \end{aligned} \quad (3)$$

where we have taken into account the symmetry properties of nucleon-nucleon amplitude in the expression (1).

The IA stands for the deuteron break-up amplitude represented by only the term in the eq.(3) with the minimal virtuality of the intermediate nucleon. It corresponds to the minimal momentum of nucleon spectator in the deuteron at rest frame. Under the kinematical conditions of the Saclay experiment it was the undetected neutron (p_3).

In the next subsections we describe the nucleon-nucleon amplitude and the deuteron wave function.

1.1 NN amplitude

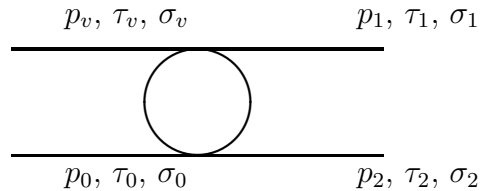


Figure 2: NN amplitude

The spin and isospin dependent NN amplitude looks like

$$M_{NN\tau_0,\tau_v;\sigma_0\sigma_v}^{\tau_1,\tau_2;\sigma_1\sigma_2}(p_1, p_2; p_0, p_v) = \frac{e^{\tau_1}e^{\tau_2} - e^{\tau_2}e^{\tau_1}}{2} M_0^{\sigma_1\sigma_2}(p_1, p_2; p_0, p_v) + \frac{e^{\tau_1}e^{\tau_2} + e^{\tau_2}e^{\tau_1}}{2} M_1^{\sigma_1\sigma_2}(p_1, p_2; p_0, p_v) ,$$

where e is the unit two by two operator in the isotopic space and the M_0 and M_1 are the isosinglet and isotriplet parts of the NN amplitude, respectively. According to the Pauli principle

the amplitudes M_0 and M_1 obey the symmetry relations

$$M_0^{\sigma_1\sigma_2}_{\sigma_0\sigma_v}(p_1, p_2; p_0, p_v) = M_0^{\sigma_2\sigma_1}_{\sigma_0\sigma_v}(p_2, p_1; p_0, p_v) ,$$

$$M_1^{\sigma_1\sigma_2}_{\sigma_0\sigma_v}(p_1, p_2; p_0, p_v) = -M_1^{\sigma_2\sigma_1}_{\sigma_0\sigma_v}(p_2, p_1; p_0, p_v) .$$

The c.m. canonical amplitudes, i.e. the S -matrix elements, of the NN scattering are expressed in terms of five complex amplitudes a, b, c, d, e [19]

$$S = \frac{1}{2}[(a+b)+(a-b)\hat{n}\otimes\hat{n}+(c+d)\hat{m}\otimes\hat{m}+(c-d)\hat{l}\otimes\hat{l}+e(e\otimes\hat{n}+\hat{n}\otimes e)] ,$$

where

$$\vec{m} = \frac{\vec{k}_f - \vec{k}_i}{|\vec{k}_f - \vec{k}_i|} , \quad \vec{l} = \frac{\vec{k}_f + \vec{k}_i}{|\vec{k}_f + \vec{k}_i|} , \quad \vec{n} = \frac{\vec{k}_i \times \vec{k}_f}{|\vec{k}_i \times \vec{k}_f|} ,$$

$\vec{k}_{i,f}$ are the initial and final c.m. momenta of the NN interacting system and $\hat{n} \equiv \vec{n} \cdot \vec{\sigma}$ and so on. The shorthand $A \otimes B$ stands for $A^{\sigma_1}_{\sigma_v} B^{\sigma_2}_{\sigma_0}$.

We have to deal with the NN amplitudes in the laboratory frame and it is inconvenient to make the transformations from numerous individual NN c.m. frames to these frame during the calculations. It is why the applying of the M-functions of Stapp [17, 18] is very natural in such calculations. The basic M-functions analogous to the S -matrix basis $e \otimes e, \hat{m} \otimes \hat{m}, \hat{l} \otimes \hat{l}, \hat{n} \otimes \hat{n}, e \otimes \hat{n} + \hat{n} \otimes e$ are built from the products $\tilde{V}_i V_j$ of the two by two (hermitian) matrices $\tilde{V}_i \equiv V_i^\mu \tilde{\sigma}_\mu$ and $V_j \equiv V_j^\mu \sigma_\mu$, where V_i^μ are the four-velocities of the scattered nucleons completed by the four-velocity V of the whole system in the arbitrary frame. The possible M-function's basis $b_i, i = 1, \dots, 6$ is given by the eqs.(28-31) of the Appendix. Once fixed, the basis allows represent the M-function of the NN scattering as a sum

$$M = g_1 b_1 + g_2 b_2 + g_3 b_3 + g_4 b_4 + g_5 \frac{b_5 + b_6}{\sqrt{2}} , \quad (4)$$

where g_i are the five complex amplitudes. The relations between the M-function's amplitudes g_i and the canonical amplitudes a, b, c, d, e are [20]

$$\begin{aligned} g_1 &= -\frac{c+d}{2}, & g_2 &= -\frac{c-d}{2}, \\ g_3 &= \frac{b+a\cos\varphi - ie\sin\varphi}{2}, & g_4 &= \frac{b-a\cos\varphi + ie\sin\varphi}{2}, \\ g_5 &= -\frac{a\sin\varphi + ie\cos\varphi}{\sqrt{2}}, & e^{i\varphi} &= \frac{\omega_0 - \omega}{\omega_0 - \omega^{-1}}, \end{aligned}$$

where $\omega = e^{i\theta}$, θ being the c.m. scattering angle, and

$$\omega_0 \equiv \sqrt{\frac{(V, V_2) + 1}{(V, V_2) - 1} \frac{(V, V_0) + 1}{(V, V_0) - 1}}.$$

The values of the amplitudes a, b, c, d, e for given laboratory energy and c.m. angle were calculated by use of the PSA of Arndt et al. [21]. The normalization of the M-functions is such that the c.m. cross-section is equal to

$$\frac{d\sigma}{d\Omega_{NN}} = \frac{1}{(8\pi)^2 s} \frac{Tr(M \tilde{V}_v \otimes \tilde{V}_0 M^\dagger V_1 \otimes V_2)}{4}.$$

The presence of metric matrices \tilde{V}_i and V_j is the peculiarity of the Stapp formalism as was mentioned in the Introduction.

As to the virtual nucleons they are off-shell and we took it into account only kinematically. In particular we calculate the basis M-functions b_i by use of the eqs.(28-31) using the 'virtual' velocity $V_v = (p_d - p_3)/m_v$, if of course $m_v^2 = (p_d - p_3)^2$ was happened to be positive. When it was not the case we assigned to the matrix elements of the corresponding nucleon-nucleon amplitude zero values. For the scalar amplitudes g_i the only

way to obtain the off-shell values is the model calculations and they are permanently in progress (see for example [22]). Still the situation is far from being satisfactory, especially for the energies above several hundreds MeV. Thus only the on-shell amplitudes obtained in the PSA are of the practical use. The choice of the on-shell kinematic corresponding to the off-shell one is ambiguous. One way is to take the PSA solution at the $s = (p_0 + p_v)^2 = (p_1 + p_2)^2$ and $t = (p_1 - p_0)^2 = (p_2 - p_v)^2$. It means to take $g_i(s, t, m_v^2) = g_i(s, t, m^2)$. Another way is to put at first the virtual nucleon on the mass-shell $p_v = (E_v, \mathbf{p}_v) \rightarrow p_v^* = (\sqrt{\mathbf{p}_v^2 + m^2}, \mathbf{p}_v)$, and then get the *PSA* solution at the $s^* = (p_0 + p_v^*)^2 \geq s$ and $t^* = (p_2 - p_v^*)^2$, i.e. to accept that $g_i(s, t, m_v^2) = g_i(s^*, t^*, m^2)$. We preferred the first way, since it ignores the off-shell mass dependence at all in contrast to the non-dynamical recipe for such dependence induced by the second way.

1.2 Deuteron wave function

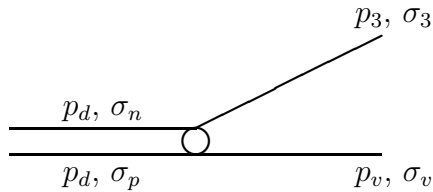


Figure 3: DNP-vertex

The DNN-vertex (see Fig. 3) relates to the wave function by

the eq.(2). The antisymmetric tensor

$$\epsilon^{\tau_v \tau_3} = \frac{1}{\sqrt{2}} \begin{pmatrix} 0 & 1 \\ -1 & 0 \end{pmatrix}$$

determines the isosinglet nature of the deuteron. The classic deuteron wave functions are related to the deuteron at rest frame. The most suitable for the transition to the M-function expression looks like

$$\Phi_{s\sigma_p\sigma_n}^{\sigma_v\sigma_3}(\vec{k}) = a(e_{\sigma_p}^{\sigma_v}e_{\sigma_n}^{\sigma_3} + e_{\sigma_n}^{\sigma_v}e_{\sigma_p}^{\sigma_3}) - bk^i k^j (e_{i\sigma_p}^{\sigma_v}e_{j\sigma_n}^{\sigma_3} + e_{i\sigma_n}^{\sigma_v}e_{j\sigma_p}^{\sigma_3}) ,$$

where subscript s reminds the S -matrix origin of the classic wave function and the unit vector \vec{k} is directed along the nucleon momentum. The matrices e_i , $i = 1, 2, 3$ coincide with the Pauli matrices, but we use the different notation to distinguish them from the matrices σ^i , which have another spinor indices: σ_{cd}^i . The scalar functions a and b are connected with the S - and D -wave functions u and w as following

$$\begin{aligned} a &= u - \frac{w}{\sqrt{8}} , & b &= -\frac{3w}{\sqrt{8}} , \\ u &= a - \frac{b}{3} , & w &= -\frac{b\sqrt{8}}{3} . \end{aligned} \quad (5)$$

The corresponding M-function of the deuteron wave function in an arbitrary frame is built from the products $\tilde{V}_v V_d$ and $\tilde{V}_3 V_d$ of the two by two matrices, where $V_{d,v,3}^\mu$ are the four-velocities of the deuteron, virtual nucleon and on-shell nucleon, respectively. It is equal to

$$\begin{aligned} \Phi_{\sigma_p\sigma_n}^{\sigma_v\sigma_3}(p_v, p_3; p_d) &= \\ a \frac{(e + \tilde{V}_v V_d)_{\sigma_p}^{\sigma_v} (e + \tilde{V}_3 V_d)_{\sigma_n}^{\sigma_3} + (e + \tilde{V}_v V_d)_{\sigma_n}^{\sigma_v} (e + \tilde{V}_3 V_d)_{\sigma_p}^{\sigma_3}}{2\sqrt{((V_v, V_d) + 1)((V_3, V_d) + 1)}} + \end{aligned}$$

$$b \frac{(e - \tilde{V}_v V_d)_{\sigma_p}^{\sigma_v} (e - \tilde{V}_3 V_d)_{\sigma_n}^{\sigma_3} + (e - \tilde{V}_v V_d)_{\sigma_n}^{\sigma_v} (e - \tilde{V}_3 V_d)_{\sigma_p}^{\sigma_3}}{2\sqrt{((V_v, V_d) - 1)((V_3, V_d) - 1)}} . \quad (6)$$

The following normalization equation holds

$$Tr(\Phi \tilde{\rho}_0 \Phi^\dagger V_3 \otimes V_v) = \Phi_{\sigma_p \sigma_n}^{\sigma_v \sigma_3} \rho_0^{\sigma_p \bar{\sigma}_p} \rho_0^{\sigma_n \bar{\sigma}_n} \bar{\Phi}_{\bar{\sigma}_p \bar{\sigma}_n}^{\bar{\sigma}_v \bar{\sigma}_3} V_{3 \bar{\sigma}_3 \sigma_3} V_{v \bar{\sigma}_v \sigma_v} = u^2 + w^2 ,$$

where $\tilde{\rho}_0$ is the invariant density matrix of the deuteron defined in the Section 4 (see eq.(19)). The functions u and w obtained with the Paris [23] or Bonn [24] potentials are approximated by series of the poles

$$\begin{aligned} u(m_d^2, m_v^2) &= \sqrt{8\pi m_d} N_S \left(\frac{1}{q^2 + \alpha^2} - \sum_i \frac{c_i}{q^2 + \alpha_i^2} \right) , \\ w(m_d^2, m_v^2) &= \sqrt{8\pi m_d} N_D \left(\frac{1}{q^2 + \alpha^2} - \sum_i \frac{d_i}{q^2 + \alpha_i^2} \right) . \end{aligned} \quad (7)$$

The values $N_{S,D}$ are the normalization constants ($N_S^2 \simeq 0.16 \text{ GeV}$) and the dependence on the m_d^2 and m_v^2 goes through the 3-momentum of the nucleons in the deuteron at rest frame

$$q = \frac{\sqrt{[(m_d + m)^2 - m_v^2][(m_d - m)^2 - m_v^2]}}{2m_d} .$$

The binding energy ϵ relates to the α as $\alpha^2 = \epsilon m$. The sum rules $\sum_i c_i = \sum_i d_i = 1$ should be fulfilled. The dimension of the wave functions u and w is GeV^{-1} and they are normalized as follows

$$\int d\vec{q} (u^2 + w^2) = (2\pi)^3 2m_d .$$

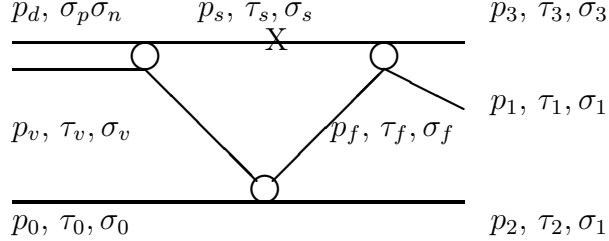


Figure 4: Double-scattering mechanism

2 NN double-scattering

Let us start with the graph shown in Fig. 4 referred to in what follows as the DS graph 2(31). Two other graphs with the cyclically permuted nucleons will be referred to as the DS graphs 1(23) and 3(12). For the DS graph 2(31) the amplitude with the 'spectator' on the mass-shell looks like

$$\begin{aligned}
 M_{DS}^{2(31)\tau_1\tau_2\tau_3;\sigma_1\sigma_2\sigma_3}_{\tau_0\tau_1\tau_2\tau_3;\sigma_0\sigma_p\sigma_n}(p_1, p_2, p_3; p_0, p_d) &= -i \int \frac{d\mathbf{p}_s}{(2\pi)^3 2E_s} \\
 M_{\tau_f\tau_s;\sigma_f\sigma_s}^{\tau_3\tau_1;\sigma_3\sigma_1}(p_3, p_1; p_s, p_{31} - p_s) M_{\tau_0\tau_v;\sigma_0\sigma_v}^{\tau_2\tau_f;\sigma_2\sigma_f}(p_2, p_{31} - p_s; p_0, p_d - p_s) & \\
 \frac{\epsilon^{\tau_v\tau_s} \Phi_{\sigma_p\sigma_n}^{\sigma_v\sigma_s}(p_d - p_s, p_s; p_d)}{2m_f(m_f - m + i\varepsilon)} &
 \end{aligned}
 \quad (8)$$

where $p_{31} = p_3 + p_1 = (E_{31}, \mathbf{p}_{31})$, $E_s = \sqrt{m^2 + \mathbf{p}_s^2}$ and $m_f^2 = (p_{31} - p_s)^2$. The simplifications are necessary to calculate of the integral (8) since it requires a knowledge of the off-shell nucleon-nucleon amplitudes. The most simple method is to take the nucleon-nucleon amplitudes out of the integral sign. Reasonable to do it at some momentum p_s^0 placed on the singular surface of the integral corresponding to the mass-shell of the virtual nucleon f . With the z -axis directed along the momentum

\mathbf{p}_{31} the equation of this surface looks like

$$\left(\frac{p_s^x}{q_{31}}\right)^2 + \left(\frac{p_s^y}{q_{31}}\right)^2 + \left(\frac{p_s^z - \frac{|\mathbf{p}_{31}|}{2}}{q_{31} \frac{E_{31}}{W_{31}}}\right)^2 = 1, \quad (9)$$

where $W_{31} = \sqrt{s_{31}} = \sqrt{p_{31}^2}$ is the invariant mass of the 31-pair of the nucleons and $q_{31} = \sqrt{s_{31} - 4m^2}/2$ is their c.m. momentum. At the end of this Section and in the Section 5 presenting the calculation results we return to the problem of the choice of this Fermi momentum.

When the nucleon pair at the final state has the invariant mass near the nucleon-nucleon threshold it is necessary and possible to take into account the off-shell behavior of the corresponding NN amplitude in the eq.(8) to fulfill the closure sum rules in the 1S_3 state (see an argumentation in [25, 26, 27]). Near the threshold it is possible to describe this off-shell behavior by the simple form-factor $M^{off} = M^{on} f(s_{31}, m_f^2)$, which is related to the 1S_3 wave function of the deuteron (7) as follows

$$f(s_{31}, m_f^2) = 1 - (q^2 + \alpha^2) \sum_i \frac{c_i}{q^2 + \alpha_i^2}, \quad (10)$$

where the dependence on the virtual mass and energy goes from the c.m. momentum

$$q = \frac{\sqrt{[(W_{31} + m)^2 - m_f^2][(W_{31} - m)^2 - m_f^2]}}{2W_{31}}.$$

We used the form-factor (10) up to the energy 200 MeV and above this energy we were replacing it by the unity. Note that at the low energies the corresponding DS graph is referred to as the final state interaction (FSI) graph.

Taking the NN amplitudes out of the integral sign, but keeping inside of it the off-shell form-factor, deuteron wave function

and the propagator, we derive the following approximation of the DS amplitude from the eq.(8)

$$\begin{aligned}
& M_{DS}^{2(31)\tau_1\tau_2\tau_3;\sigma_1\sigma_2\sigma_3}(\tau_0; \sigma_0\sigma_p\sigma_n)(p_1, p_2, p_3; p_0, p_d) \simeq \\
& -i\epsilon^{\tau_v\tau_s} M_{\tau_f\tau_s;\sigma_f\sigma_s}^{\tau_3\tau_1;\sigma_3\sigma_1}(p_3, p_1; p_s^0, p_{31} - p_s^0) M_{\tau_0\tau_v;\sigma_0\sigma_v}^{\tau_2\tau_f;\sigma_2\sigma_f}(p_2, p_{31} - p_s^0; p_0, p_d - p_s^0) \\
& F_{\sigma_p\sigma_n}^{\sigma_v\sigma_s}(s_{31}, t_2) ,
\end{aligned} \tag{11}$$

where

$$F_{\sigma_p\sigma_n}^{\sigma_v\sigma_s}(s_{31}, t_2) \equiv \int \frac{d\mathbf{p}_s}{(2\pi)^3 2E_s} \frac{\Phi_{\sigma_p\sigma_n}^{\sigma_v\sigma_s}(p_d - p_s, p_s; p_d) f(s_{31}, (p_{31} - p_s)^2)}{2m_f(m_f - m + i\epsilon)}$$

and $t_2 = (p_2 - p_0)^2 = (p_d - p_{31})^2$. The deuteron wave function Φ is defined by the eq.(6). To preserve the covariance it is necessary to approximate the velocities of the virtual nucleon (v) and the nucleon 'spectator' (s) in the latter integral by the corresponding values in the NN amplitudes taken out of the integral sign. Then the expression for the F becomes

$$\begin{aligned}
F_{\sigma_p\sigma_n}^{\sigma_v\sigma_s}(s_{31}, t_2) \simeq & \frac{F_a}{2} \frac{(e + \tilde{V}_v V_d)_{\sigma_p}^{\sigma_v} (e + \tilde{V}_s V_d)_{\sigma_n}^{\sigma_s} + (e + \tilde{V}_v V_d)_{\sigma_n}^{\sigma_v} (e + \tilde{V}_s V_d)_{\sigma_p}^{\sigma_s}}{2\sqrt{((V_v, V_d) + 1)((V_s, V_d) + 1)}} + \\
& \frac{F_b}{2} \frac{(e - \tilde{V}_v V_d)_{\sigma_p}^{\sigma_v} (e - \tilde{V}_s V_d)_{\sigma_n}^{\sigma_s} + (e - \tilde{V}_v V_d)_{\sigma_n}^{\sigma_v} (e - \tilde{V}_s V_d)_{\sigma_p}^{\sigma_s}}{2\sqrt{((V_v, V_d) - 1)((V_s, V_d) - 1)}},
\end{aligned}$$

where

$$V_v = \frac{p_d - p_s^0}{\sqrt{(p_d - p_s^0)^2}}, \quad V_s = \frac{p_s^0}{m}, \quad V_d = \frac{p_d}{m_d}$$

are the four-velocities of the corresponding particles. The complex functions $F_{a,b}$ are equal to (see eqs.(5))

$$F_a = F_u - \frac{F_w}{\sqrt{8}}, \quad F_b = -\frac{3F_w}{\sqrt{8}},$$

where

$$F_u(s_{31}, t_2) \equiv \int \frac{d\mathbf{p}_s}{(2\pi)^3 2E_s} \frac{u(m_d^2, (p_d - p_s)^2) f(s_{31}, (p_{31} - p_s)^2)}{2m_f(m_f - m + i\varepsilon)}$$

and F_w is determined analogously by the w -wave function. For the pole expansion of the functions u and w (7) a good analytical approximation of these integrals have been obtained by J.M.Laget [28]:

$$\begin{aligned} F_u \simeq & \frac{N_S}{q_{31}\sqrt{32\pi m_d}} \{ \\ & 2 \left[\arctan \frac{p_+}{\alpha} + \arctan \frac{p_-}{\alpha} - \sum_i c_i \left(\arctan \frac{p_+}{\alpha_i} + \arctan \frac{p_-}{\alpha_i} \right) \right] \\ & + 4 \left[\sum_i c_i \arctan \frac{q_{31}}{2(\alpha + \alpha_i)} - \sum_{i,j} c_i c_j \arctan \frac{q_{31}}{2(\alpha_i + \alpha_j)} \right] \quad (12) \\ & i \left[\ln \frac{p_-^2 + \alpha^2}{p_+^2 + \alpha^2} - \sum_i c_i \ln \frac{p_-^2 + \alpha_i^2}{p_+^2 + \alpha_i^2} \right] \} , \end{aligned}$$

where

$$q_{31} = \frac{\sqrt{[(W_{31} + m_d)^2 - t_2][(W_{31} - m_d)^2 - t_2]}}{2m_d}$$

is the momentum of 31-pair in the deuteron at rest frame and

$$p_{\pm} \equiv \frac{q_{31}}{2} \pm \frac{s_{31} + m_d^2 - t_2}{2W_{31}m_d} \frac{\sqrt{s_{31} - 4m^2}}{2} .$$

The replacements in the eq.(12) of the normalization constant N_S by the N_D and of the parameters c_i by the d_i entail the expression for the F_w . We have tried in the calculations the F_w thus obtained in addition to the F_u , but in the final calculations it was still omitted. The reason for this lays in the closure sum

rule, which requires in case of the $F_w \neq 0$ to take into account the off-shell behavior of the FSI nucleon-nucleon amplitude also in the 1D_3 -state, rather than in the 1S_3 -state only as we did.

The real part of the factor F in the eq.(12) has two terms. The first one is due to the off-shell states contribution inside the triangle loop, which is proved to be canceled in the eikonal regime [13]. The second term in the real part (12) originates from the threshold form factor (10) and we were dropping it for the energies of the finally interacting nucleons above 200 MeV.

Now let us return to the problem of the choice of the Fermi momentum p_s^0 in the eq.(11). We have considered two candidates. The first one is advocated as follows. The deuteron wave function in the integral (8) drops quickly with the decreasing of the virtual mass $m_v^2 = (p_d - p_s)^2$ suppressing by this the contribution of \mathbf{p}_s corresponding to the small virtual masses m_v . It is reasonable then to test the p_s^0 giving the maximum value of m_v . In the c.m. frame of the 31-pair the momenta placed on the ellipsoidal surface (9) look like $(\frac{W_{13}}{2}, q_{31}\mathbf{n})$, where \mathbf{n} is an unite vector. Then

$$m_v^2 = (p_d - p_s^0)^2 = m_d^2 + m^2 - E_d W_{13} + 2p_d q_{31} x ,$$

where (E_d, \mathbf{p}_d) is the deuteron four-momentum in this frame and x is the cosine of the angle between \mathbf{n} and \mathbf{p}_d . Therefore the maximum m_v^2 is achieved at $x = 1$ and the momentum of the nucleon s should be directed along the deuteron momentum in the 31-pair c.m. frame. We will denote the momentum thus obtained as p_s^{max} . The argumentation for the second candidate is less evident and consists of the following. Since the states with small virtual masses are still contribute to the integral (8) we should not use the Fermi momentum corresponding to the maximal m_v but try a momentum corresponding to some smaller

value of the virtual mass m_v . We have chosen for this purpose the momentum placed at the 'top' of the ellipsoidal surface (9), which corresponds to the maximum velocity of the nucleon s in the laboratory frame. We will call this momentum as the optimal one and will denote it as p_s^{opt} . With the z -axis directed along the momentum \mathbf{p}_{31} its components are

$$p_s^{opt} = (E_s, 0, 0, \frac{|\mathbf{p}_{13}|}{2} + q_{31} \frac{E_{13}}{W_{13}}) ,$$

whereas the momentum p_s^{max} has in this frame the components

$$p_s^{max} = (E_s, q_{31}n_x, q_{31}n_y, \frac{|\mathbf{p}_{13}|}{2} + q_{31} \frac{E_{13}}{W_{13}}n_z) ,$$

where \mathbf{n} is the unite vector directed along the deuteron momentum in c.m. frame of the 31-pair.

The comparison with the experiment of the calculations performed using the both Fermi momenta is presented in the Section 5 and definitely testifies in favor of the optimal Fermi momentum p_s^{opt} .

3 Δ -excitation contribution

The contribution corresponding to the graph shown in Fig. 5 is equal to

$$\begin{aligned} M_{\Delta}^{2(31)\tau_1\tau_2\tau_3;\sigma_1\sigma_2\sigma_3}_{\tau_0 \quad ;\sigma_0\sigma_p\sigma_n}(p_1, p_2, p_3; p_0, p_d) = \\ i \frac{\Gamma^{t\tau_2;\sigma_2}_{\tau_0;\sigma_0}(p_2, q; p_0) M_t^{\tau_1\tau_3;\sigma_1\sigma_3}_{;\sigma_p\sigma_n}(p_1, p_3; q, p_d)}{q^2 - \mu^2} , \quad q = p_0 - p_2 , \quad (13) \end{aligned}$$

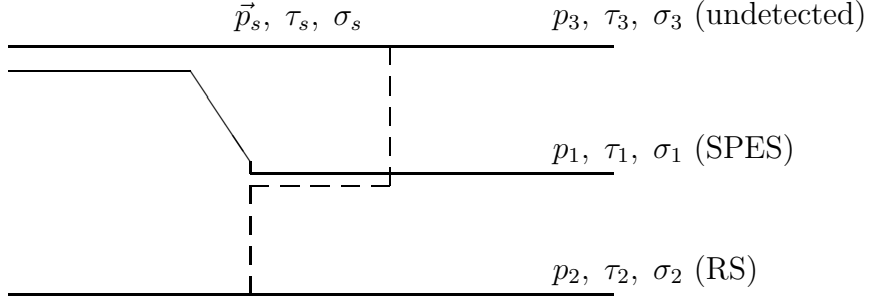


Figure 5: Δ excitation mechanism

where the μ is the pion mass. The πNN -vertex in the eq.(13) is equal to

$$\Gamma_{\tau_0; \sigma_0}^{t\tau_2; \sigma_2}(p_2, q; p_0) = e^{t\tau_2} G_{\sigma_0}^{\sigma_2}(p_2, q; p_0) ,$$

where t is the isovector index of the pion and

$$e^{+1} = \begin{pmatrix} 0 & 0 \\ 1 & 0 \end{pmatrix} , \quad e^{-1} = \begin{pmatrix} 0 & 1 \\ 0 & 0 \end{pmatrix} , \quad e^0 = \frac{1}{\sqrt{2}} \begin{pmatrix} 1 & 0 \\ 0 & -1 \end{pmatrix} .$$

The spatial part of πNN -vertex with the virtual pion looks in Stapp formalism like (see the eq.(26) of the Appendix)

$$G_{\sigma_0}^{\sigma_2}(p_2, q; p_0) = f(q^2) g_\pi m (e - \tilde{V}_2 V_0)_{\sigma_0}^{\sigma_2} ,$$

where $g_\pi \simeq 13.6$ is the πNN coupling constant, and $f(q^2)$ is the pion form factor, for which we took the monopole representation

$$f(q^2) = \frac{m_\pi^2 - \Lambda^2}{q^2 - \Lambda^2} \quad (14)$$

with the cut-off $\Lambda = 1.0$ GeV.

The spin and isospin dependent $\pi d \rightarrow \text{NN}$ amplitude in the eq.(13) looks like

$$M_t^{\tau_1 \tau_3; \sigma_1 \sigma_3}_{;\sigma_p \sigma_n}(p_1, p_3; q, p_d) = \epsilon_t^{\tau_1 \tau_3} M_{\sigma_p \sigma_n}^{\sigma_1 \sigma_3}(p_1, p_3; q, p_d) ,$$

where

$$\epsilon_{+1} = \begin{pmatrix} 1 & 0 \\ 0 & 0 \end{pmatrix}, \quad \epsilon_{-1} = \begin{pmatrix} 0 & 0 \\ 0 & -1 \end{pmatrix}, \quad \epsilon_0 = -\frac{1}{\sqrt{2}} \begin{pmatrix} 0 & 1 \\ 1 & 0 \end{pmatrix}.$$

The amplitudes of the physical reactions are equal then to

$$M_{\pi^+ d \rightarrow pp} = M, \quad M_{\pi^- d \rightarrow nn} = -M, \quad M_{\pi^0 d \rightarrow np} = -\frac{M}{\sqrt{2}}.$$

We have used for the deriving of the M-function of the $\pi d \rightarrow \text{NN}$ reaction the S -matrix elements obtained by J.M.Laget [29]. In this approach the one-loop box diagrams with the $N\Delta$ as the intermediate state had been calculated numerically, including the πN intermediate scattering in the S, P and D waves parametrized by their phase shifts. However, to avoid the double counting with the DS term we have excluded the P_{11} -wave (the nucleon pole in the πN amplitude is a part of the DS term). Finally, the ρ -exchange was considered in the $\pi d \rightarrow \text{NN}$ amplitude. The details are given in the Appendix of the paper [29]. These calculations have been performed in the deuteron at rest frame.

So having at our disposal the S -matrix elements

$$S_{\sigma_p \sigma_n}^{\sigma_1 \sigma_3}(p_{1(d)}, p_{3(d)}; q_{(d)}, m_d),$$

where the subscript (d) means that the momenta are considered in the deuteron at rest frame, we have to obtain the M-function in an arbitrary frame. The only way in this case is the straightforward applying of the common recipe prescribed by the eq.(23) of the Appendix. At first we derive the M-function in the deuteron at rest system:

$$M_{\sigma_p \sigma_n}^{\sigma_1 \sigma_3}(p_{1(d)}, p_{3(d)}; q_{(d)}, m_d) = v_1^{\sigma_1} v_{3b}^{\sigma_3} S_{\sigma_p \sigma_n}^{a \ b}(p_{1(d)}, p_{3(d)}; q_{(d)}, m_d). \quad (15)$$

The boost matrix v_b^a of the nucleon from the rest to the four-velocity $(V_0, \mathbf{k}\sqrt{V_0^2 - 1})$, where \mathbf{k} is the unit vector along the momentum, is determined by the eq.(24). Having obtained the M-matrix in the deuteron at rest frame we applied to the eq.(15) the boost transformation v_{d0}^a corresponding to the deuteron moving along the z -axis with the four-velocity $(V_{d0}, 0, 0, \sqrt{V_{d0}^2 - 1})$ so that the final M-function looked like (see the eq.(25))

$$M_{\sigma_p \sigma_n}^{\sigma_1 \sigma_3}(p_1, p_3; q, p_d) = v_{d0}^{\sigma_1} v_{d0}^{\sigma_3} M_g^a{}_h(p_{1(d)}, p_{1(d)}; q_{(d)}, m_d) v_d^{-1g}{}_{\sigma_p} v_d^{-1h}{}_{\sigma_n} .$$

4 Deuteron density matrix and observables

Let us remind at first how like looks the density matrix of a spinor particle in the Stapp formalism [18]:

$$\rho^{a\bar{b}} = \frac{1}{2}(V^\mu + S^\mu)\sigma_\mu^{a\bar{b}} , \quad (16)$$

where the $a, b = 1, 2$ are the spinor indices, V^μ is the four-velocity and S^μ is the four-vector of polarization of the particle, which is orthogonal to V : $(V, S) = 0$. In the index-less form it looks like

$$\tilde{\rho} = \frac{1}{2}(V^\mu + S^\mu)\tilde{\sigma}_\mu = \frac{1}{2}(\tilde{V} + \tilde{S}) .$$

The analog of the expression (16) for the vector particle is

$$\rho^{\sigma_p \bar{\sigma}_p \sigma_n \bar{\sigma}_n} = \rho^{\mu\nu} \sigma_\mu^{\sigma_p \bar{\sigma}_p} \sigma_\nu^{\sigma_n \bar{\sigma}_n} , \quad (17)$$

where

$$\rho^{\mu\nu} = \frac{1}{12} \left[-g^{\mu\nu} + 4V^\mu V^\nu + 2\sqrt{3}(S^\mu V^\nu + S^\nu V^\mu) + 4\sqrt{\frac{3}{2}}T^{\mu\nu} \right] .$$

The S and T are the vector and tensor polarizations with the properties

$$(S, V) = 0, \quad T^{\mu\nu} = T^{\nu\mu}, \quad V_\mu T^{\mu\nu} = 0, \quad T_\mu^\mu = 0.$$

In the index-less form eq.(17) could be written as

$$\tilde{\rho} = \rho^{\mu\nu} \tilde{\sigma}_\mu \otimes \tilde{\sigma}_\nu.$$

If the quantization axis is directed along the y -axis then in the c.m. frame we have

$$S = (0, 0, \frac{\sqrt{3}}{2} p_y, 0),$$

$$T = -\frac{p_{yy}}{2\sqrt{6}} \begin{pmatrix} 0 & 0 & 0 & 0 \\ 0 & 1 & 0 & 0 \\ 0 & 0 & -2 & 0 \\ 0 & 0 & 0 & 1 \end{pmatrix},$$

where $p_y \equiv n_+ - n_-$ and $p_{yy} \equiv n_+ + n_- - 2n_0$. The statistical weights n_+, n_-, n_0 of the states with the definite projections of the spin on the quantization axis are normalized so that $n_+ + n_0 + n_- = 1$. Then $Tr(\rho^2) = n_+^2 + n_0^2 + n_-^2$. If the particle moves along the z -axis with the velocity $V = (V_0, 0, 0, V_z)$, then S does not change, but T becomes

$$T_{\mu\nu} = -\frac{p_{yy}}{2\sqrt{6}} \begin{pmatrix} V_z^2 & 0 & 0 & V_0 V_z \\ 0 & 1 & 0 & 0 \\ 0 & 0 & -2 & 0 \\ V_0 V_z & 0 & 0 & V_0^2 \end{pmatrix} \equiv -\frac{p_{yy}}{2\sqrt{6}} t_{\mu\nu}.$$

We can represent then the $\tilde{\rho}$ as

$$\tilde{\rho}_d = \tilde{\rho}_0 + \frac{3}{2} p_y \tilde{\rho}_y + \frac{1}{2} p_{yy} \tilde{\rho}_{yy}, \quad (18)$$

where

$$\tilde{\rho}_0 \equiv \frac{1}{3} \tilde{V} \otimes \tilde{V} - \frac{1}{12} \tilde{\sigma}_\mu \otimes \tilde{\sigma}^\mu \quad (19)$$

is the unpolarized density matrix and

$$\begin{aligned} \tilde{\rho}_y &\equiv -\frac{1}{3} (\tilde{\sigma}_y \otimes \tilde{V} + \tilde{V} \otimes \tilde{\sigma}_y) , \\ \tilde{\rho}_{yy} &\equiv -\frac{1}{6} t_{\mu\nu} \tilde{\sigma}^\mu \otimes \tilde{\sigma}^\nu \end{aligned}$$

are the vector and the tensor polarization matrices, respectively. If the (target) proton is unpolarized, the initial density matrix of the dp system is equal to

$$\tilde{\rho}_i = \frac{\tilde{V}_0}{2} \otimes \tilde{\rho}_d$$

and the vector and tensor analyzing powers are equal to

$$\sigma_0 A_y = \frac{Tr(M \tilde{V}_0 \otimes \tilde{\rho}_y \ M^\dagger \ V_1 \otimes V_2 \otimes V_3)}{2} , \quad (20)$$

$$\sigma_0 A_{yy} = \frac{Tr(M \tilde{V}_0 \otimes \tilde{\rho}_{yy} \ M^\dagger \ V_1 \otimes V_2 \otimes V_3)}{2} , \quad (21)$$

where

$$\sigma_0 \equiv \frac{Tr(M \tilde{V}_0 \otimes \tilde{\rho}_0 \ M^\dagger \ V_1 \otimes V_2 \otimes V_3)}{2}$$

is the unpolarized cross section. The polarization of the fast outgoing nucleon in the y direction is determined by the equation

$$\sigma P_{1y} = Tr(M \tilde{\rho}_i \ M^\dagger \ \sigma^y \otimes V_2 \otimes V_3) ,$$

where the polarized cross section is equal to

$$\sigma = Tr(M \tilde{\rho}_i \ M^\dagger \ V_1 \otimes V_2 \otimes V_3) = \sigma_0 \left(1 + \frac{3}{2} p_y A_y + \frac{1}{2} p_{yy} A_{yy} \right) .$$

The last equation follows from the eqs.(18,20,21). Introducing the polarization P_0 of this nucleon for the unpolarized deuteron and the depolarization parameters D_v as follows

$$\sigma_0 P_0 = \frac{Tr(M \tilde{V}_0 \otimes \tilde{\rho}_0 M^\dagger \sigma^y \otimes V_2 \otimes V_3)}{2},$$

$$\sigma_0 D_v = \frac{Tr(M \tilde{V}_0 \otimes \tilde{\rho}_y M^\dagger \sigma^y \otimes V_2 \otimes V_3)}{2}$$

we can write polarization P_{1y} for the vector polarized deuteron beam in the following form

$$P_{1y} = \frac{P_0 + \frac{3}{2}p_y D_v}{1 + \frac{3}{2}p_y A_y}. \quad (22)$$

5 Calculation results and discussion

Let us start with the main parameters of the detecting system of the performed experiment. Polarized deuteron beam of the accelerator Saturne was incident on a 4 cm thick liquid hydrogen target. Fast protons from the reaction (p_1) were selected at the scattering angle $\Theta_1 = 18.0 \pm 0.5^\circ$ by the magnetic spectrometer SPES-4 in the coincidence with the recoil protons (p_2) detected at the angle $\Theta_2 = 57.0^\circ (\pm 4.25^\circ$ in the scattering plane and $\pm 8^\circ$ in the vertical plane) with a mosaic of E and ΔE scintillation counters. Two multiwire proportional chambers at 1.5 and 3 m from the target provided the recoil proton track position. Six central momentum settings for the proton detected in SPES-4 ($p_{10} = 1.6, 1.7, 1.8, 1.9, 2.0, 2.05$ GeV/c) were studied. The polarimeter POMME located behind the final focal plane of

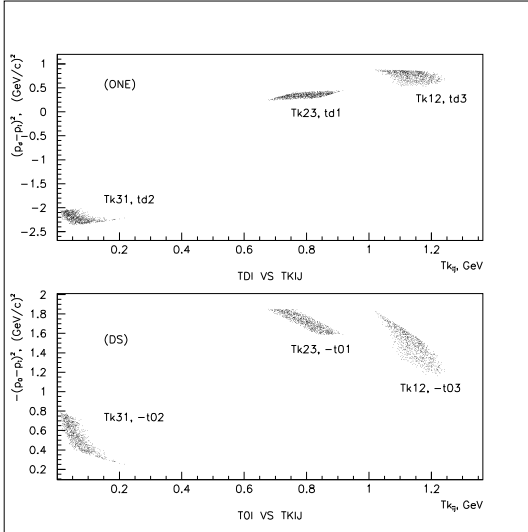


Figure 6: The (T_{ij}, t_{di}) and (T_{ij}, t_{0i}) distributions for $p_{10} = 1.6$ GeV/c and HES.

SPES-4 was used to measure the polarization of the fast protons. At the chosen Θ_1 and for the momentum p_1 of the fast proton, two kinematic solutions are possible for the recoil proton energy T_2 , which according to our definition are the high energy (HES) and the low energy (LES) solutions. The neutron spectator momenta in the deuteron rest frame, denoted as q , ranged from 30 to 440 MeV/c.

Thus the calculation procedure should include scanning over the acceptance of the detecting system. By scanning over the allowed phase space of the detectors, we intended to obtain a realistic calculation result, which can be directly compared to the data. This scanning procedure inevitably invokes the necessity for a Monte-Carlo type event generation, because the number of phase unit volumes amounts to a huge number when the unit volume is defined by the resolution of the measurement.

We would like to show now, taking the $p_{10} = 1.6$ GeV/c and HES as an example, some kinematic distributions characterizing different mechanisms of the deuteron break-up in this experiment. In Fig. 6 the two-dimensional distributions of the kinetic energies $T_{ij} = (s_{ij} - 4m^2)/2m$ of the i, j pairs of the final nucleons with two momenta transfer, $t_{di} = (p_d - p_i)^2$ and $t_{0i} = (p_0 - p_i)^2$, are shown. Note that t_{di} are equal to the squared masses of virtual nucleon in the nucleon pole graphs. It is seen that of three final nucleons considered as the spectator in these pole graphs, the neutron (p_3) provides the maximal masses of the exchanged nucleon. The pole graph with p_2 as the spectator gives the negative squared masses and we have excluded this graph from the calculation. The distributions of (T_{ij}, t_{0i}) characterize the graphs of the DS mechanism. T_{31} ranges from 30 to 200 Mev and therefore the DS graph 2(31) is the typical FSI graph. Two other pairs of the final nucleons and especially two protons p_1 and p_2 have much higher relative energies. However applying of the Glauber approach when calculating the DS graphs with these pairs being rescattered [12, 14] is not justified because the momenta transfer t_{03} and t_{01} for these graphs are very high. Thus we have applied for calculation of the DS graphs the expression (11) and two others obtained from it by the cyclic permutation of the final nucleons.

We would like now to return to the problem mentioned in the Section 2. It is the choice of the Fermi momentum p_s^0 in the eq.(11). The dotted line in Fig. 7 presents the polarization observables calculated with the p_s^{max} in the DS graph 1(23) and with the p_s^{opt} in the DS graph 3(12) (the sensitivity of the contribution of the FSI to the choice of Fermi momentum is weak and we fixed it to be p_s^{max}). The dashed line corresponds to the

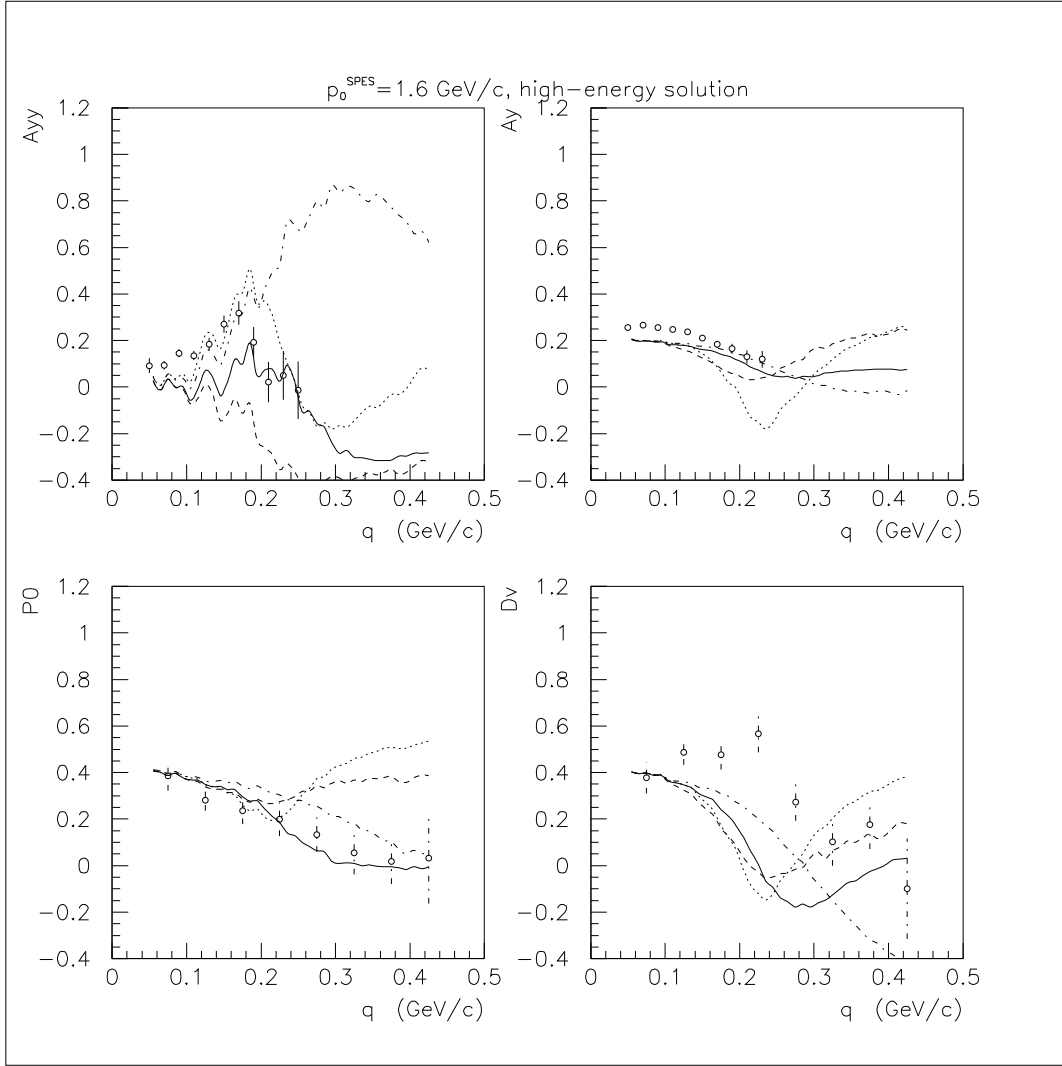


Figure 7: Polarization observables for the different choices of the Fermi momentum. Dotted line presents the calculations with p_s^{max} in the DS graph 1(23) and p_s^{opt} in the DS graph 3(12). Dashed line corresponds to the choice of p_s^{opt} for DS graph 1(23) and p_s^{max} for the DS graph 3(12). Solid line is obtained with the p_s^{opt} in the both these graphs. The dashed-dotted line presents the only FSI prediction (DS graph 2(31)).

choice of the p_s^{opt} for the DS graph 1(23) and of the p_s^{max} for the DS graph 3(12). The solid line is obtained with the p_s^{opt} in the both these graphs. The improvement in the description of the data in the latter case is evident. It is important that neglecting of these graphs results in the significant worsening of the data description. The dashed-dotted line presents the only FSI prediction and we see that it does not provide the suppression of the tensor analyzing power at the high q observed in the experiment. So we can summarize that besides the FSI graph the both 1(23) and 3(12) DS graphs are required for data description and they should be calculated with p_s^{opt} as the Fermi momentum. It is the very choice of the DS model, which we have applied in further calculations.

The measured tensor analyzing powers A_{yy} and the calculation results with Bonn deuteron wave function are shown in Figs. 8 and 9. The main feature of the experimental data is the strong deviation from the IA (dashed line) for $q \geq 0.2$ GeV/c. The full theory including the Δ -excitation graphs (full line) gives the satisfactory explanation of this deviation, the DS graphs (dashed-dotted line) playing the decisive role. One could expect the more noticeable Δ -effects taking in mind that the laboratory kinetic energies of the 23-pair of the final nucleons range from 0.7 to 0.9 GeV (see Fig. 6), which is exactly the region of the Δ dominance in the $\pi d \rightarrow NN$ amplitude. Yet the momentum transfer t_{01} from the target proton to the fast proton detected by the SPES-4 is very high and the pion form factor (14) reduces the common contribution of the graph shown in Fig. 5 (with, of course, correspondingly interchanged final nucleons).

The vector analyzing power A_y results, shown in Figs.10 and 11, exhibit the similar tendency: significant correction to the IA

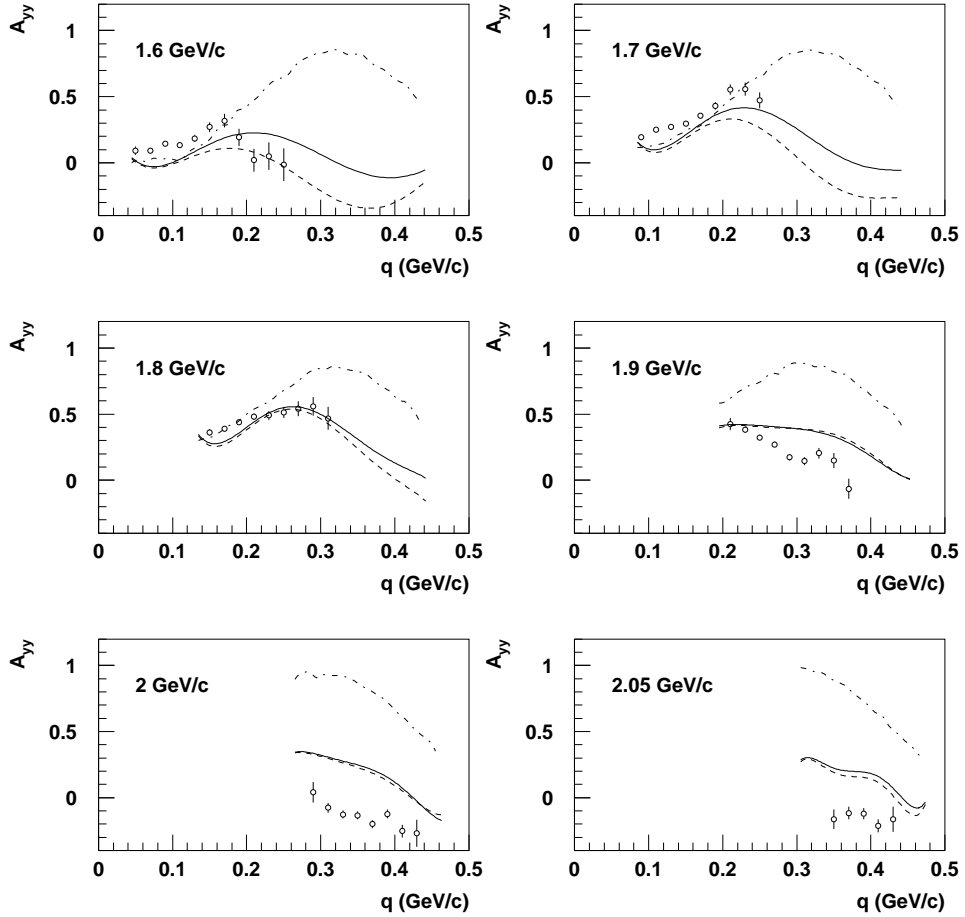


Figure 8: The tensor analyzing power A_{yy} for the HES. The experimental points are presented for the different values of the central momentum detected in the magnetic spectrometer and as a function of the outgoing neutron momentum in the deuteron at rest frame. The dashed-dotted line is the IA, the dashed line has in addition the DS contribution, and the continuous line is the full calculation including in addition the virtual Δ .

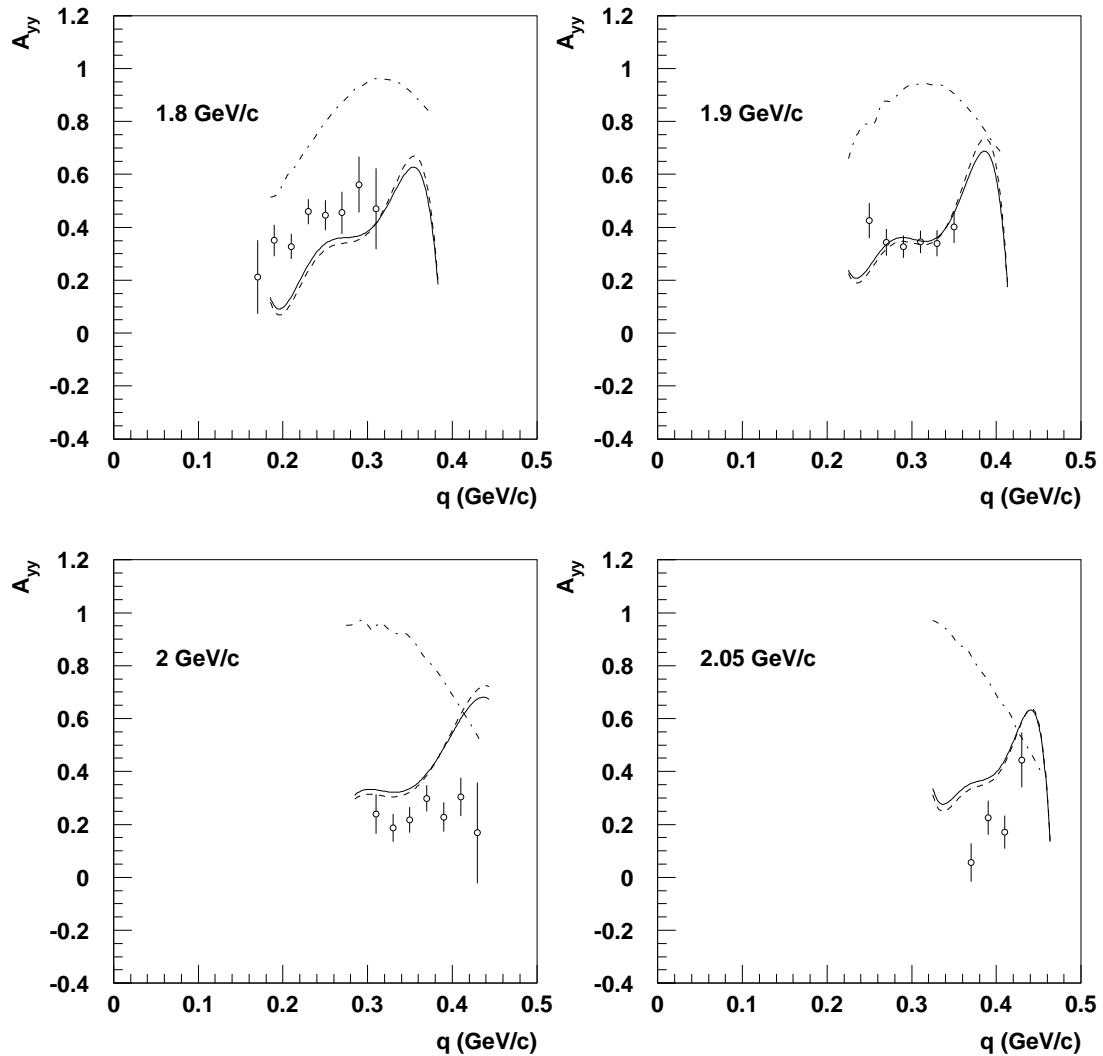


Figure 9: The tensor analyzing power A_{yy} for the LES. Same notations as in Fig. 8.

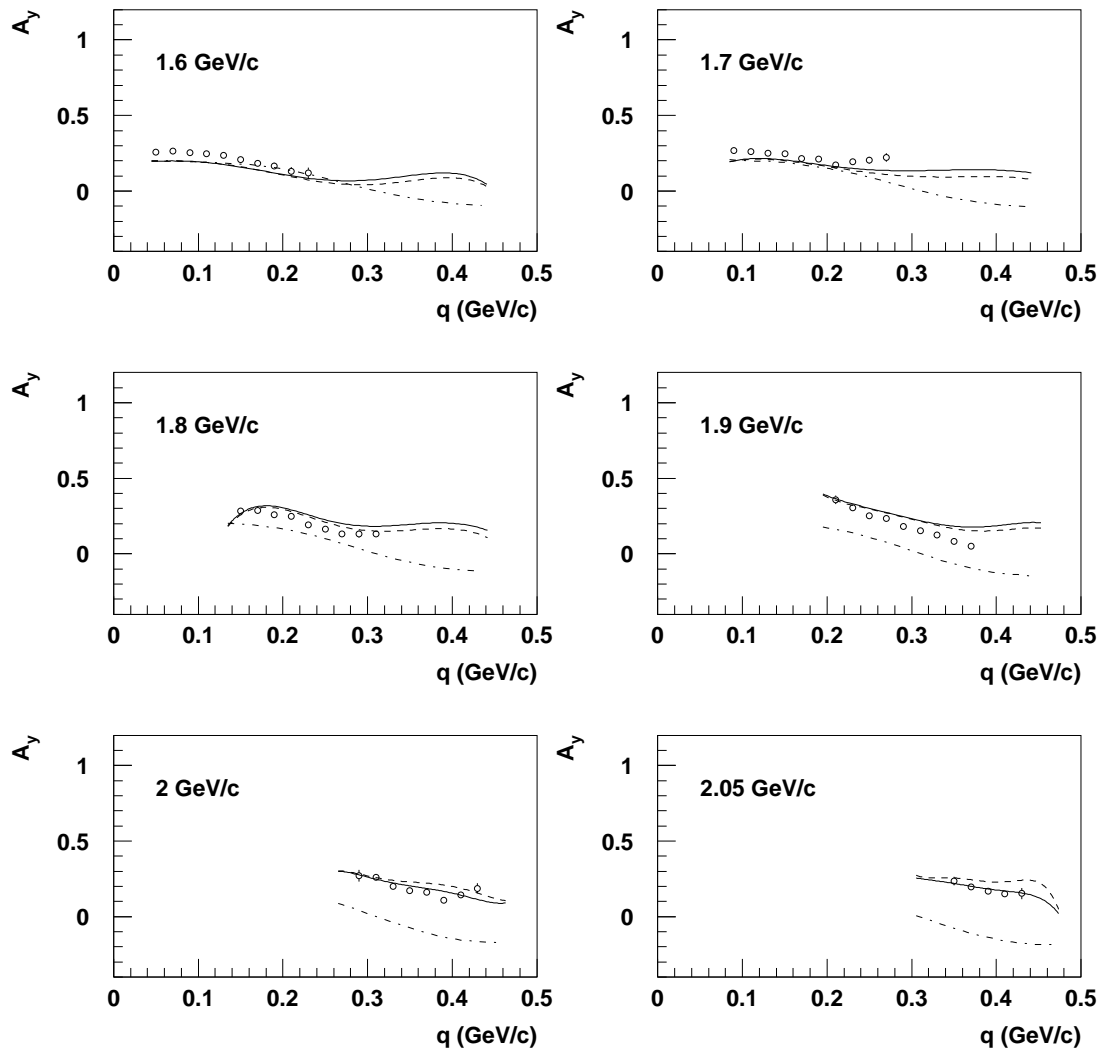


Figure 10: The vector analyzing power A_y for the HES. Same notations as in Fig. 8.

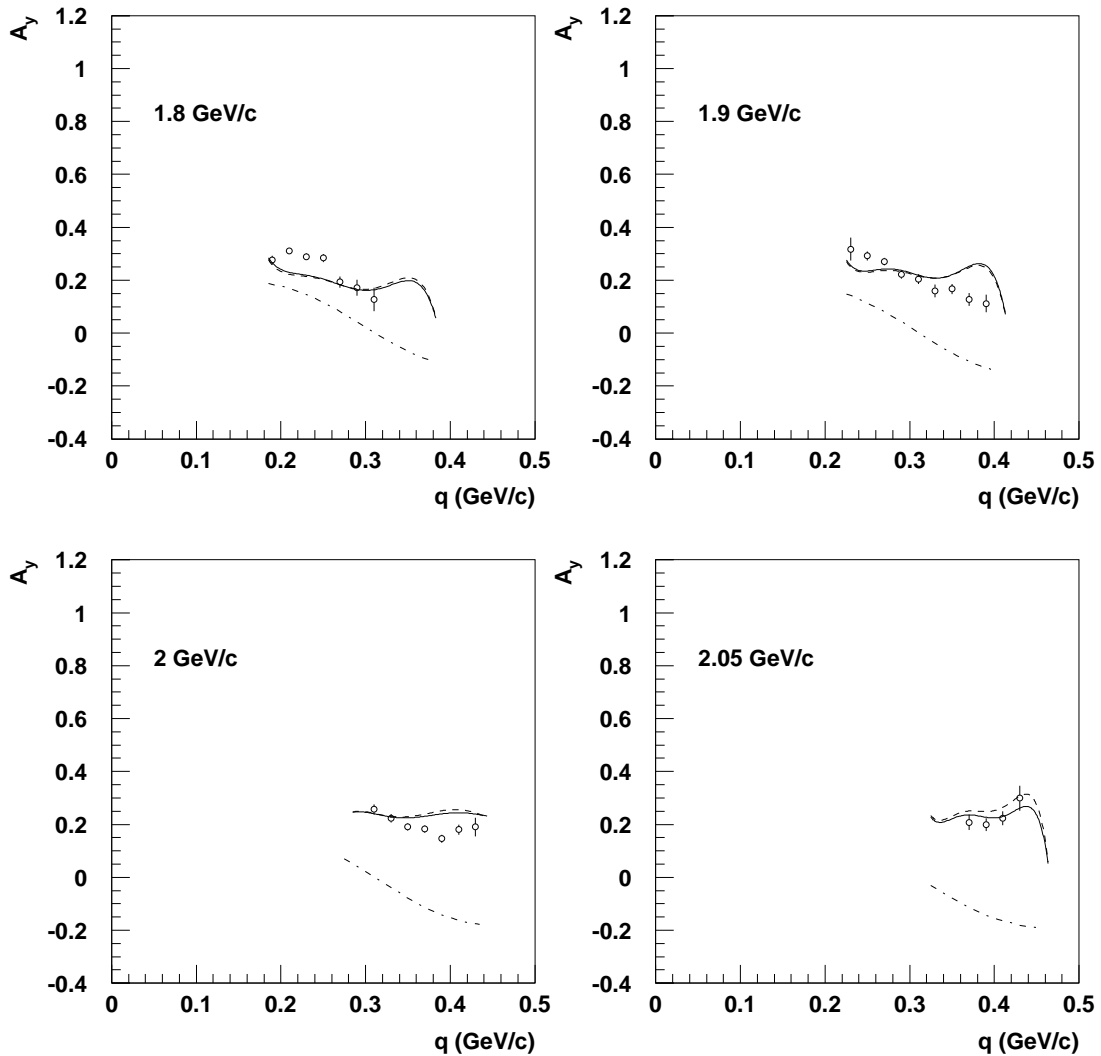


Figure 11: The vector analyzing power A_y for the LES. Same notations as in Fig. 8.

above 0.25 GeV/c by the full calculations. The surprisingly good coincidence, taking in mind the very small statistical errors of the measured values, of full calculations with the experimental points is achieved at the all SPES-4 settings for the both high and low energy solutions.

For the polarization of the fast proton the data are averaged over the SPES-4 settings to obtain more statistics. However the calculations were performed for each setting. The experimental data and the calculations are presented in the terms of the proton polarization P_0 for the unpolarized deuteron and the depolarization parameters D_v (see the eq.(22)) and are shown in Figs.12-13 and 14, respectively. For HES a good description is obtained for the P_0 with the full diagram calculations, whereas it is not the case for LES. For the D_v , the IA is even closer to the data than the full calculations. However, considering the large error bars for the D_v , one can say that there is not decisive discrimination between the both calculations.

The above results were obtained with the Bonn deuteron wave function [24]. Returning to the initial idea of this experiment to discriminate between the different deuteron wave functions we have tried also widely used Paris deuteron wave function [23]. In Fig. 15 the results of the calculations for the both wave functions at 1.8 and 2.0 GeV/c settings of the SPES-4 are shown. It is seen that the dependence on the deuteron wave function of the full calculations is weak.

To conclude we would like to remind that the main task of this experiment was the investigation of the deuteron structure in the high internal momentum region. The polarization data were thought to bring the information on the S - and D -component of the deuteron wave function, which would be possible only if the

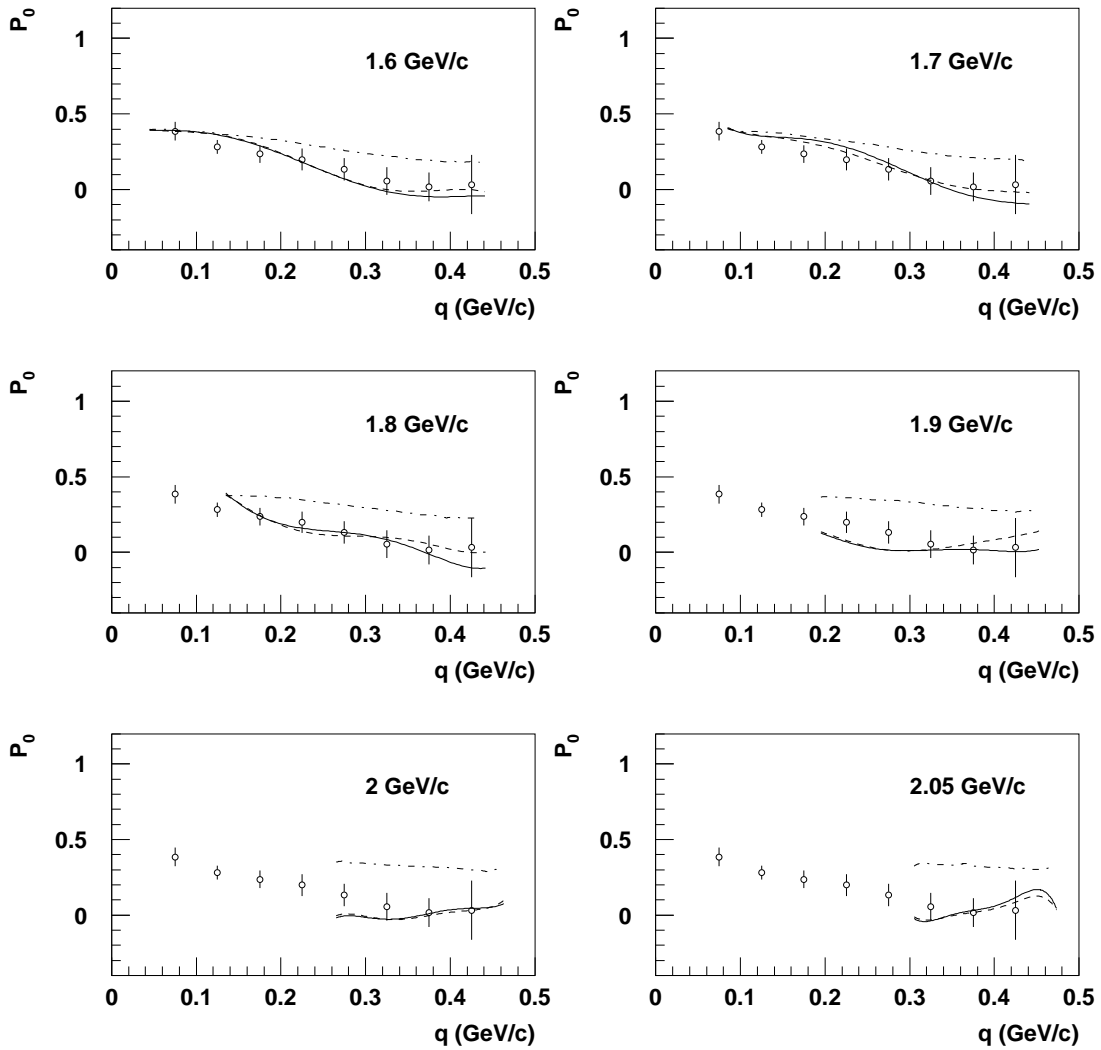


Figure 12: The forward proton polarization P_0 for the HES. The notation of the curves are the same as in Fig. 8. The calculations are done consistently as for A_y and A_{yy} for each setting of the spectrometer while the data are summed.

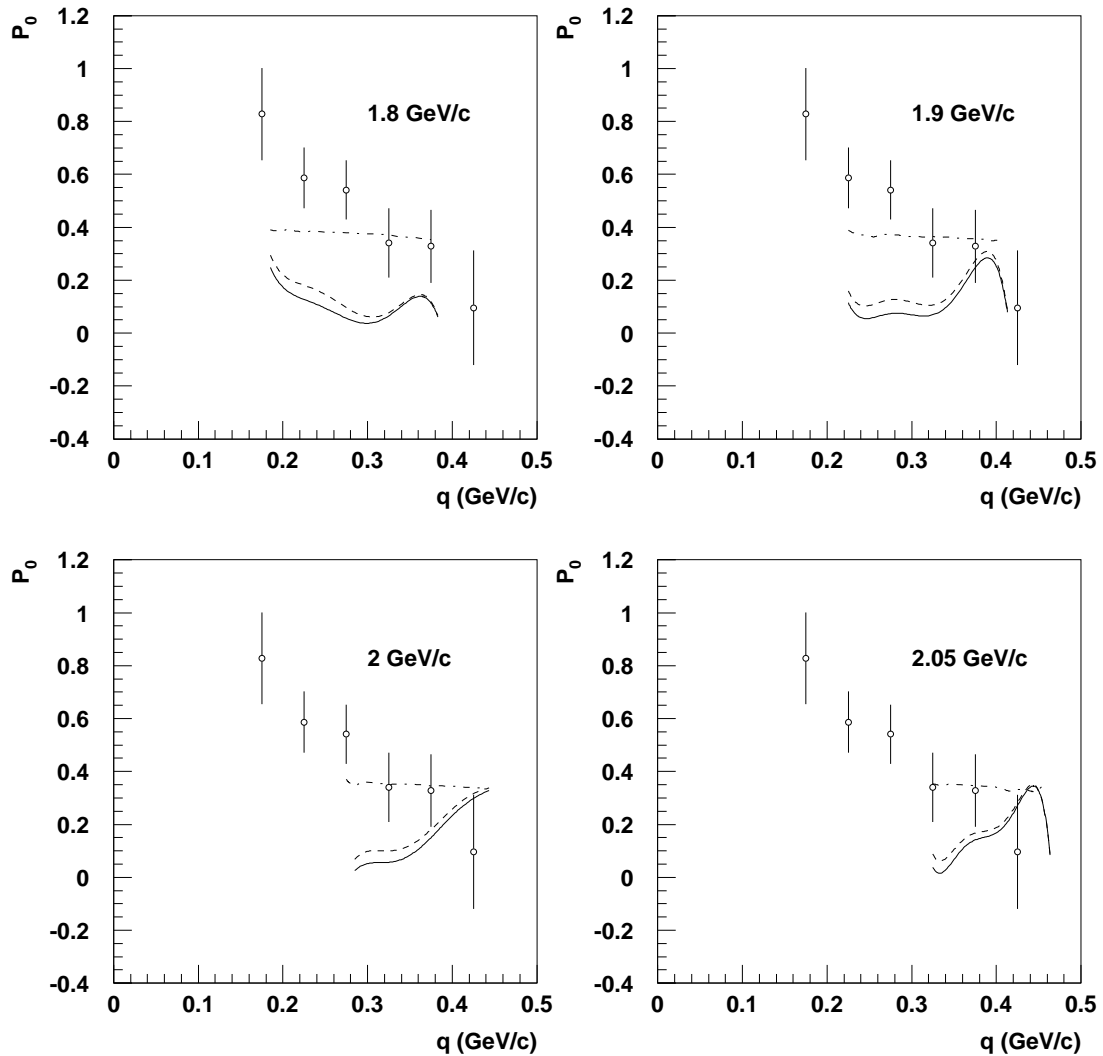


Figure 13: The forward proton polarization P_0 for the LES. The notation of the curves are the same as in Fig. 8.

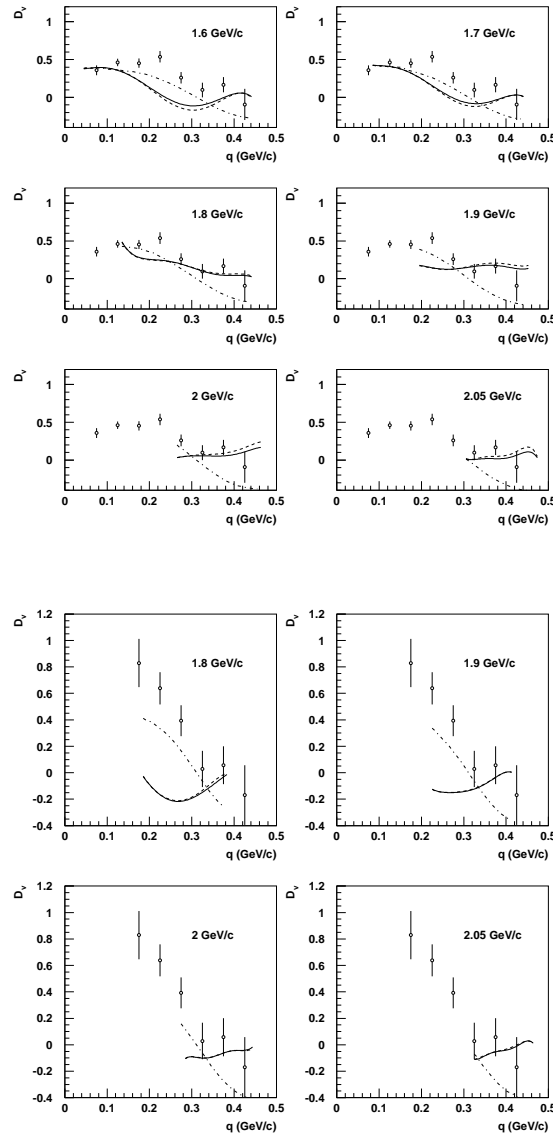


Figure 14: The depolarization parameter D_v for the HES (right picture) and LES (left picture) . Same notations as in Fig. 8.

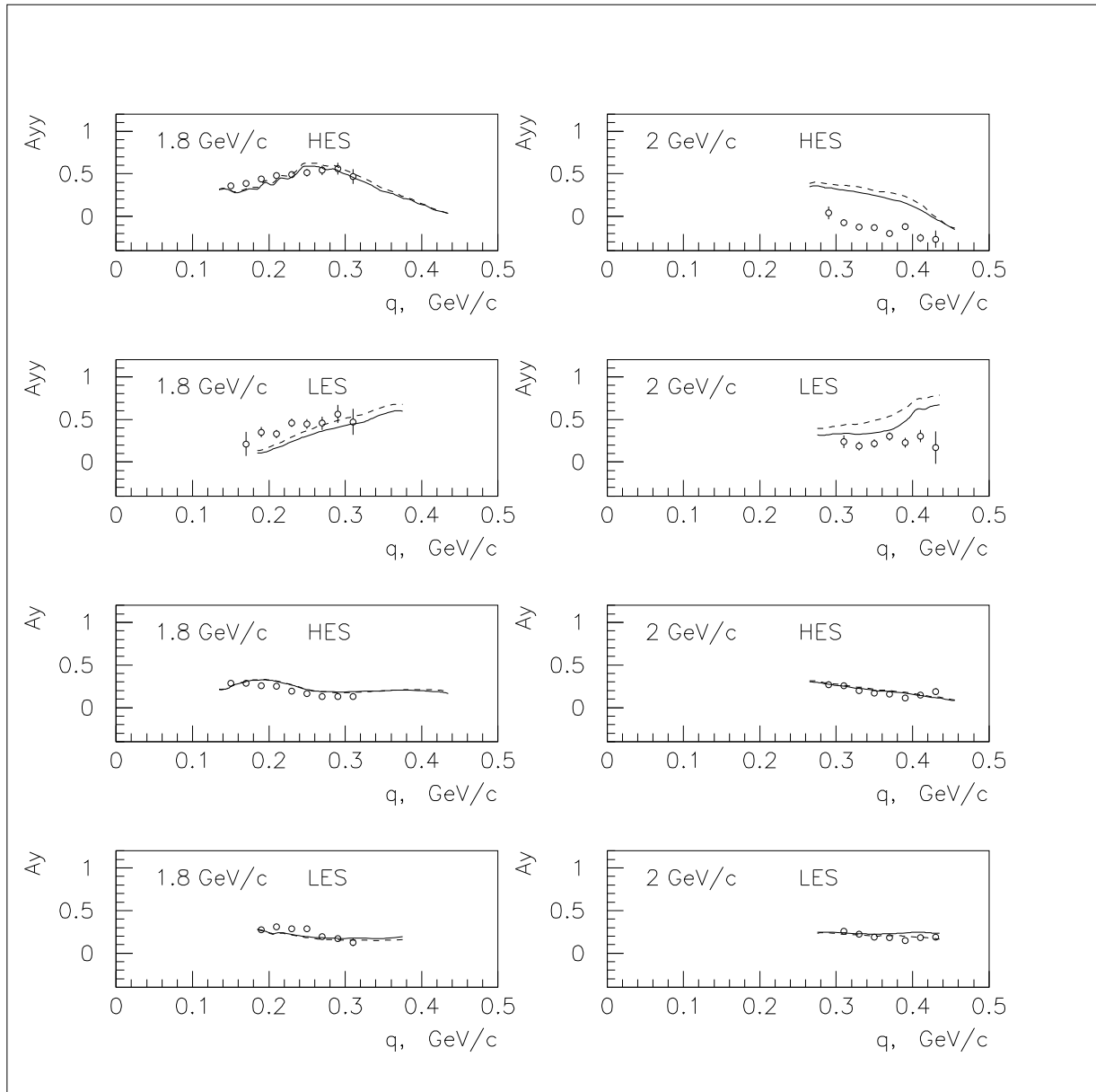


Figure 15: Comparison of the Bonn(full line) and Paris(dashed line) deuteron wave functions predictions

IA would dominate in the reaction mechanism. The underlying idea of this experiment as well as the analogous ones is that the deviations from the IA, corrected by other presumably small contributing conventional mechanisms, could be interpreted as the revealing of the quark degrees of freedom. In fact, the polarization parameters, measured at first time in this exclusive experiment with a large accuracy and in a large amount, deviate strongly from the IA at the high internal momenta. However, the estimations of other traditional reaction mechanisms, the nucleon-nucleon double-scattering being the most significant, were tried and have shown a qualitative agreement to the referred experimental data. This agreement between the data and the theory is thought to imply that the possible new degrees of freedom in the deuteron structure contribute much smaller than the hadronic degrees. Still definite perfection of the model is necessary for the adequate description of the polarized deuteron break-up data. Investigation of the short range deuteron wave function, if it is at all possible in the deuteron break-up experiments with the hadron probes, will be, by our opinion, the further step only after all discrepancies in theoretical description of polarization observables are overcome.

Acknowledgements

The author thanks S.Belostotski, A.Boudard, J.-M.Laget and V.Nikulin for fruitful discussions and cooperation during performing this work. He is also very grateful to A.Boudard for the warm hospitality at Service de Physique Nucleaire, Centre d'Etudes de Saclay, where the main part of this work was done.

Appendix. M-functions

Let us consider the process with the n_f and n_i spinor particles in the final and initial channels, respectively. We will denote the corresponding amplitude with the indices as

$$M^{\sigma_{1_f} \dots \sigma_{n_f}}{}_{\sigma_{1_i} \dots \sigma_{n_i}} .$$

Let v_i be the boosts of i -th spinor particle moving with the velocity V_i . Then the connection between the S -matrix and M-function looks like

$$S = v_{1_f}^{-1} \otimes \dots \otimes v_{n_f}^{-1} M v_{1_i} \otimes \dots \otimes v_{n_i} . \quad (23)$$

The boost matrix v_b^a from the rest to the 4-velocity $(V_0, \mathbf{k}\sqrt{V_0^2 - 1})$, where \mathbf{k} is the unit vector along the momentum, is equal to

$$v_b^a = \begin{pmatrix} v_0 + v_3 & v_1 - iv_2 \\ v_1 + iv_2 & v_0 - v_3 \end{pmatrix} , \quad (24)$$

where

$$v = \frac{1}{\sqrt{2}}(\sqrt{V_0 + 1}, \mathbf{k}\sqrt{V_0 - 1}) .$$

With respect to Lorentz transformations, represented by the unimodular matrices z

$$z_b^a = \begin{pmatrix} z_0 + iz_3 & iz_1 + z_2 \\ iz_1 - z_2 & z_0 - iz_3 \end{pmatrix} ,$$

where $z_{0,1,2,3}$ are the complex numbers such that $z_0^2 + z_1^2 + z_2^2 + z_3^2 = 1$, the M-functions behave as the operators in the direct product of spinor spaces

$$M \rightarrow z \otimes \dots \otimes z M z^{-1} \otimes \dots \otimes z^{-1} . \quad (25)$$

The simplicity of the transformation (25) is the main advantage of the M-functions. It allows to build the M-functions from products $\tilde{V}_i V_j$ of two by two matrices $\tilde{V}_i \equiv V_i^\mu \tilde{\sigma}_\mu$ and $V_j \equiv V_j^\mu \sigma_\mu$, where V_i^μ are the four-velocities of the scattered spinor particles completed by the four-velocity V of the whole system in the arbitrary frame. The matrices $\sigma^\mu = (1, \vec{\sigma})$ and $\tilde{\sigma}^\mu = (1, -\vec{\sigma})$, where $\vec{\sigma}$ are the standard Pauli matrices, have the different position of spinor indices specified in the following way

$$\sigma^\mu \rightarrow \sigma_{\bar{a}b}^\mu, \quad \tilde{\sigma}^\mu \rightarrow \sigma^{\mu a \bar{b}}.$$

The simplest M-functions are easy to derive using the Dirac bispinors in the Weyl representation in the M-function form

$$u^\alpha{}_b = \sqrt{m} \begin{pmatrix} e_b^a \\ V_{\bar{a}b} \end{pmatrix}, \quad \bar{u}_\alpha^b = \sqrt{m} \begin{pmatrix} e_a^b & V^{b\bar{a}} \end{pmatrix}.$$

Here α is the bispinor index, $V_{\bar{a}b} = V_\mu \sigma_{\bar{a}b}^\mu$, $V^{b\bar{a}} = V_\mu \sigma^{\mu b \bar{a}}$ and V_μ is the four-velocity of the particle. Let us consider for example the πNN vertex. In the Weyl representation the γ_5 -matrix looks like

$$\gamma_5 = \begin{pmatrix} e & 0 \\ 0 & -e \end{pmatrix}$$

and the amplitude of the transition between real nucleons with the production of the pion is equal to

$$M_b^a(p_f, q; p_i) = g_\pi \bar{u}_\alpha^a \gamma_5^\alpha \sigma_b^\beta u_\beta^b = g_\pi m (e_b^a - V_f^{a\bar{c}} V_{i\bar{c}b}),$$

or in the index-less form

$$M(p_f, q; p_i) = g_\pi \bar{u}_f \gamma_5 u_i = g_\pi m (e - \tilde{V}_f V_i). \quad (26)$$

The matrices \tilde{V}_i and V_i , where V_i^μ is the four-velocity of the i -th particle, serve as the metric tensors for the spin index of this

particle in Stapp formalism when performing the contraction over this index (traces, successive processes). So, in contrast to the simple expression of the cross section via the S -matrix elements

$$\sigma = \frac{1}{2^{n_i}} \text{Tr}(SS^\dagger) ,$$

the same via the M -functions looks like

$$\sigma = \frac{1}{2^{n_i}} M_{\sigma_{1_i} \dots \sigma_{n_i}}^{\sigma_{1_f} \dots \sigma_{n_f}} V_{1_i}^{\sigma_{1_i} \bar{\sigma}_{1_i}} \dots V_{n_i}^{\sigma_{n_i} \bar{\sigma}_{n_i}} M_{\bar{\sigma}_{1_i} \dots \bar{\sigma}_{n_i}}^{\bar{\sigma}_{1_f} \dots \bar{\sigma}_{n_f}} V_{1_f}^{\bar{\sigma}_{1_f} \sigma_{1_f}} \dots V_{n_f}^{\bar{\sigma}_{n_f} \sigma_{n_f}} ,$$

or in the index-less form

$$\sigma = \frac{1}{2^{n_i}} \text{Tr}(M \tilde{V}_{1_i} \otimes \dots \otimes \tilde{V}_{n_i} M^\dagger V_{1_f} \otimes \dots \otimes V_{n_f}) . \quad (27)$$

At last let us give one of the basis of the M -functions for the NN scattering. It is convenient to use such functions b_i in the development (4), that the cross section is equal to $\sum_i |g_i|^2$. From the eq.(27) follows that for this purpose one should build the basis orthonormalized with respect to the scalar product

$$(M_i, M_j) \equiv \frac{\text{Sp}(M_i \tilde{V}_0 \otimes \tilde{V}_v M_j^\dagger V_1 \otimes V_2)}{4} .$$

The eqs.(28-31) present such a basis [20]

$$b_i \equiv \frac{M_i}{\sqrt{\|M_i\|^2}} , i = 1 \dots 6 , \quad (28)$$

where

$$\begin{aligned} M_1 &= (e - \tilde{V}_1 V_v) \otimes (e - \tilde{V}_2 V_0) . \\ M_2 &= (\tilde{V}_1 V - \tilde{V} V_v) \otimes (\tilde{V}_2 V - \tilde{V} V_0) . \\ M_3 &= (e + \tilde{V}_1 V_v) \otimes (e + \tilde{V}_2 V_0) , \\ M_4 &= (\alpha^{1v}(e + \tilde{V}_1 V_v) - (\tilde{V}_1 V + \tilde{V} V_v)) \otimes (\alpha^{20}(e + \tilde{V}_2 V_0) - (\tilde{V}_2 V + \tilde{V} V_0)) , \\ M_5 &= (e + \tilde{V}_1 V_v) \otimes (\alpha^{20}(e + \tilde{V}_2 V_0) - (\tilde{V}_2 V + \tilde{V} V_0)) , \\ M_6 &= (\alpha^{1v}(e + \tilde{V}_1 V_v) - (\tilde{V}_1 V + \tilde{V} V_v)) \otimes (e + \tilde{V}_2 V_0) , \end{aligned} \quad (29)$$

with

$$\alpha^{ij} \equiv 2 \frac{(V, V_i + V_j)}{(V_i + V_j)^2}, \quad (30)$$

and

$$\begin{aligned} \|M_1\|^2 &= 4 [1 - (V_1, V_v)] [1 - (V_2, V_0)] \\ \|M_2\|^2 &= 4 [1 + (V_1, V_v) - 2(V_1, V)(V_v, V)] [1 + (V_2, V_0) - 2(V_2, V)(V_0, V)] \\ \|M_3\|^2 &= 4 [1 + (V_1, V_v)] [1 + (V_2, V_0)] \\ \|M_4\|^2 &= \frac{\|M_5\|^2 \|M_6\|^2}{\|M_3\|^2} \\ \|M_5\|^2 &= 4 \frac{1+(V_1, V_v)}{1+(V_2, V_0)} \{ [1 - (V, V_2)^2] [1 - (V, V_0)^2] - [(V_2, V_0) - (V, V_2)(V, V_0)]^2 \} \\ \|M_6\|^2 &= 4 \frac{1+(V_2, V_0)}{1+(V_1, V_v)} \{ [1 - (V, V_1)^2] [1 - (V, V_v)^2] - [(V_1, V_v) - (V, V_1)(V, V_v)]^2 \}. \end{aligned} \quad (31)$$

The V_i in the above equations are the four-velocities of the i -th particle, V being the four-velocity of the whole NN c.m. system.

References

- [1] J.Erő et al., Phys. Rev. C50 (1994) 2687.
- [2] S.L.Belostotsky et al., Phys. Rev. C56 (1997) 50.
- [3] C.F.Perdrisat et al., Phys. Rev. 187 (1969) 1201.
- [4] T.R.Witten et al., Nucl. Phys. A254 (1975) 269.
- [5] R.D.Felder et al., Nucl. Phys. A264 (1976) 397.
- [6] C.F.Perdrisat et al., Phys. Lett. 156B (1985) 38.
- [7] N.P.Aleshin et al., Nucl. Phys. A568 (1994) 809.
- [8] M.L.Goldberger and G.F.Cheung, Phys. Rev. 87 (1952) 778.
- [9] L.D.Faddeev, Sov. Phys. JETP (1961) 1014.

- [10] A.Everett, Phys. Rev. 126 (1962) 831.
- [11] B.M.Golovin et al., Sov. J. Nucl. Phys. 16 (1973) 602.
- [12] J.M.Wallace, Phys. Rev. C5 (1972) 609.
- [13] D.R.Harrington, Phys. Rev. 184 (1969) 1745.
- [14] V.Punjabi and C.F.Perdrisat, Phys. Rev. C42 (1990) 1899.
- [15] A.F.Yano, Phys. Lett. 156B (1985) 1985.
- [16] H.Joss, Fortschr. d. Phys. 10 (1962) 65.
- [17] Henry P.Stapp, Phys. Rev. 125 (1962) 2139.
- [18] Henry P.Stapp, Phys. Rev. D27 (1983) 2445.
- [19] J.Bystritsky et al., Journ. de Physique 39 (1978) 1.
- [20] O.G.Grebnyuk, Petersburg Nuclear Physics Institute preprint 1541 (1989).
- [21] R.Arndt et al., Phys. Rev. D35 (1987) 128 .
- [22] F.Gross et al., Phys. Rev. C45 (1992) 2094.
- [23] M.Lacombe et al., Phys. Lett. 101B (1981) 139.
- [24] R.Machleidt et al., Phys. Pep. 149 (1987) 2.
- [25] B.S.Aladashvili et al., J. Phys. G:Nucl.Phys. 3 (1977) 7.
- [26] C.Wilkin and C.Alvear, J. Phys. G:Nucl.Phys. 10 (1984) 1025.
- [27] V.G.Ksenzov and V.M.Kolybasov, Sov. J. Nucl. Phys. 22 (1976) 372.

[28] J.M.Laget Nucl. Phys. A296 (1978) 389.

[29] J.M.Laget, Nucl. Phys. A370 (1981) 491.